Thermochimica Acta, 52 (1982) 31–39
Elsevier Scientific Publishing Company, Amsterdam—Printed in The Netherlands

THERMAL DECOMPOSITION STUDIES ON ETHYLXANTHATO COMPLEXES OF IRON AND NICKEL

G N. NATU, S B KULKARNI and P S DHAR

Department of Chemistry, University of Poona, Pune-411007 (India)

(Received 20 May 1981)

ABSTRACT

Thermal decompositional studies on bis-ethylxanthato-nickel(II) and tris-ethylxanthato-iron(III) were carried out leading to stoichiometric, dirty green-coloured, NiO and α-Fe_2O_3 When a mixture of the xanthato complexes containing a Ni Fe atom ratio of 1 2 was decomposed, a mixed metal oxide nickel ferrite, $NiFe_2O_4$, could be obtained at about 700°C Kinetic parameters such as the activation energy, E_a, and the order of the reaction, n, were calculated using the methods of Freeman and Carroll, Arrhenius, and Borchardt and Daniels The composition, E_a, and composition–decomposition temperature diagrams were found to be clearly indicative of the formation of a definite reaction product at a certain composition Mechanistic and non-mechanistic approaches have been compared and it was found that most of the processes were explained by the Mampel relation The characterization of the decomposition products was made using X-ray and Mössbauer studies.

INTRODUCTION

The thermal analysis of metal complexes containing sulphur ligands are rather less extensively studied. For example, tris-ethylxanthato-iron(III), $Fe(xan)_3$, has been overlooked [1] for thermal studies, may be because of its impure nature even after repeated recrystallisations. The thermal decomposition of metal xanthates yields corresponding metal sulphides and volatile organic matter, containing CS_2, COS etc. The study of volatile organic matter has been done [2] by gas chromatography and mass spectrometry. To explain the formation of gaseous products it has been proposed that the first step involves the rupture of C–S bonds producing metal sulphides and a mixture of gases. But there are few reports about the characterization of the residues containing the metal. A number of reports [3–6] may be found on the thermal decomposition of $Ni(xan)_2$. The xanthates appear to be suitable for studying the formation of metal sulphides and/or oxides because of their low decomposition temperatures compared with other complexes.

The present study hopes to elucidate more of the kinetic and mechanistic aspects of the thermal decompositions of the pure metal xanthates of nickel(II) and iron(III) and their mixtures. The data on activation energies, E_a, have been interpreted on the basis of different methods of calculations.

0040-6031/82/0000–0000/$02 75

EXPERIMENTAL

The complexes, $Fe(xan)_3$ [7,8] and $Ni(xan)_2$ [3] were prepared by the procedures reported. $Fe(xan)_3$ was recrystallised twice from diethyl ether and was used immediately for subsequent studies. The elemental analyses of the starting compounds and of the major decomposition products were performed using standard methods [9].

The TG/DTA studies were performed on the thermobalance set up in the author's laboratory [10]. The characterization of the residues were based on Mossbauer and X-ray powder studies on typical samples.

RESULTS AND DISCUSSION

The TG curve of $Ni(xan)_2$, Fig. 1, exhibits a major decomposition step between 190 and 240°C. The weight loss for this step is 70% and the residue analysed to be NiS. The second step from 650 to 700°C corresponds to a loss of 5.3% giving the stoichiometric oxide, NiO (a green amorphous powder). It was further confirmed from X-ray powder patterns.

The TG curve of $Fe(xan)_3$, Fig. 1, shows two steps. The first major decomposition step occurs in the range 110 to 140°C and the second in the range 200 to 240°C. The residues at these two steps were analysed to have the compositions FeS_3 and FeS_2, respectively.

DTA showed that the two xanthato complexes melt at low temperatures. The mixtures of the two complexes in the molten state gave a homogeneous phase as evidenced from DTA studies, Fig. 2. Further decomposition of the melt leads to the formation of mixed metal sulphides and finally to the mixed metal oxides which are normally obtained by ceramic techniques [11]. The retention of the homogeneity in the solid phase of mixed metal sulphides could be presumed because of the isomorphous nature of the iron–sulphur and nickel–sulphur systems [12]. It was considered appropriate at this stage to evaluate the energetics of these decomposition reactions since these may throw light on the kinetics and mechanism.

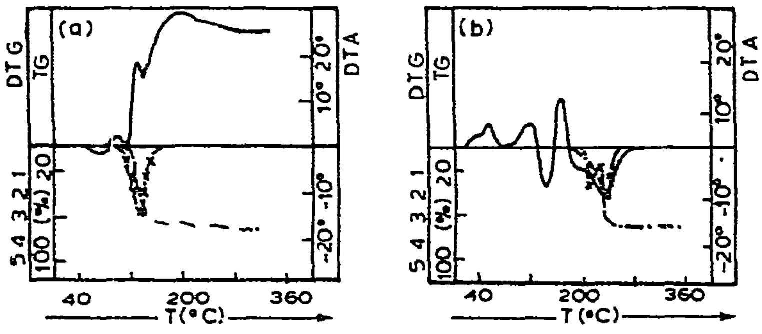

Fig 1 TG, DTG and DTA curves of (a) $Fe(xan)_3$ and (b) $Ni(xan)_2$

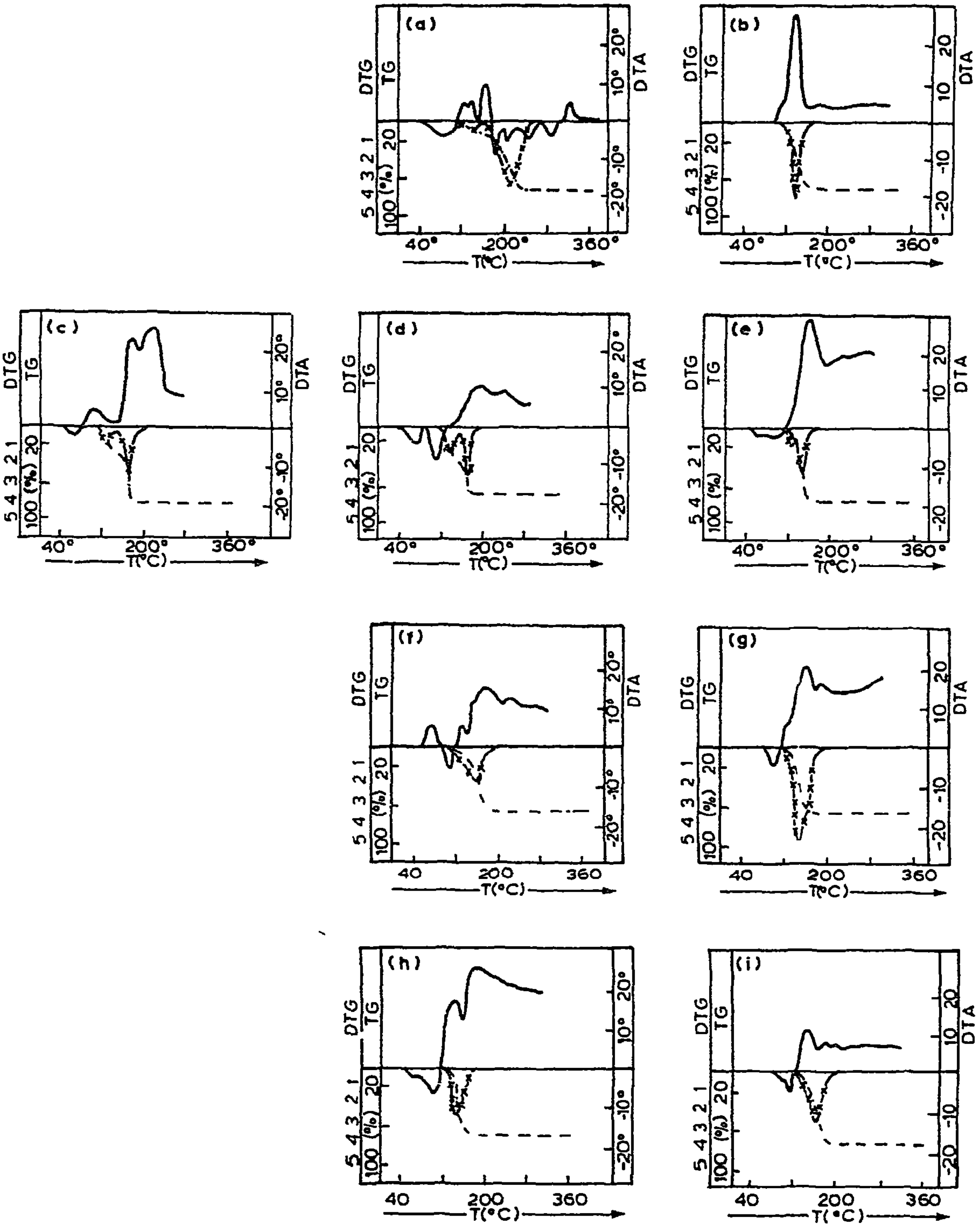

Fig 2 TG (------), DTG (X——X) and DTA (———) curves of the mixtures of complexes in varying atom percentages of Fe and Ni. (a) 10% Fe(xan)$_3$, 90% Ni(xan)$_2$, (b) 20% Fe(xan)$_3$, 80% Ni(xan)$_2$; (c) 30% Fe(xan)$_3$, 70% Ni(xan)$_2$, (d) 40% Fe(xan)$_3$, 60% Ni(xan)$_2$, (e) 50% Fe(xan)$_3$, 50% Ni(xan)$_2$, (f) 60% Fe(xan)$_3$, 40% Ni(xan)$_2$; (g) 70% Fe(xan)$_3$, 30% Ni(xan)$_2$; (h) 80% Fe(xan)$_3$, 20% Ni(xan)$_2$, (i) 90% Fe(xan)$_3$, 10% Ni(xan)$_2$.

The kinetics of this reaction has, therefore, been studied using the methods outlined by Arrhenius [13] Freeman and Carroll [14] and Borchardt and Daniels [15]. The formation of mixed metal oxides has been studied by applying the methods of thermal analysis to samples containing mixtures of complexes in varying atom percentages of the two metals. A perspective view may be obtained from the TG/DTG/DTA curves in Fig. 2 and Tables 1 and 2.

The examination of the TG/DTA curves and the characterization of the residues at different stages for pure complexes and for their mixtures reveal the following interesting observations:

(i) The first endothermic DTA peak appears at 70°C for pure Fe(xan)$_3$ and at 148°C for pure Ni(xan)$_2$. It usually corresponds to the melting of the substance or some similar change leading to the destabilization of the state of the substance. The part of the DTA curves for the mixtures containing 10 to 40% of iron show a complex multiplet structure in this region; on the other hand the mixtures containing 50 to 70% of iron do not show such a structure. This is indicative of the fact that the melting of the substance is governed mostly by the content of the low melting Fe(xan)$_3$ in the mixture. The intensity of this peak is a maximum for the pure nickel complex. The position of the endothermic change remains fairly constant at 104°C for mixtures containing over 50% iron.

(ii) The two other DTA peaks of interest are the exothermic peaks; one in the decomposition region and the other in the first plateau region of the TG curve. These two peaks appear for pure Fe(xan)$_3$ at 132 and 180°C and those for pure Ni(xan)$_2$, at 172 and 228°C. The sample containing 10% iron shows a DTA decomposition peak at 184°C which recedes towards lower temperatures with increasing iron content. The value of 152°C for the mixture containing 80% iron is slowly nearing the value of 132°C for pure Fe(xan)$_3$. The trend observed in the DTA

TABLE 1

TG Data for the Fe(xan)$_3$–Ni(xan)$_2$ system

Sample no	Composition	Temp range for loss (°C)	% Weight loss	Probable composition of the residue
1	Pure Ni(xan)$_2$	188–260	70.0	NiS
2	10% Fe(xan)$_3$ + 90% Ni(xan)$_2$	112–240	70.2	NiS + FeS$_3$
3	20% Fe(xan)$_3$ + 80% Ni(xan)$_2$	108–192	70.8	NiS + FeS$_3$
4	30% Fe(xan)$_3$ + 70% Ni(xan)$_2$	96–176	71.5	NiS + FeS$_3$
5	40% Fe(xan)$_3$ + 60% Ni(xan)$_2$	104–180	72.2	NiS + FeS$_3$
6	50% Fe(xan)$_3$ + 50% Ni(xan)$_2$	112–176	71.6	NiS + FeS$_3$
7	60% Fe(xan)$_3$ + 40% Ni(xan)$_2$	104–172	64.07	NiS + FeS$_3$
8	70% Fe(xan)$_3$ + 30% Ni(xan)$_2$	120–180	65.4	NiS + FeS$_3$
9	80% Fe(xan)$_3$ + 20% Ni(xan)$_2$	128–200	68.2	NiS + FeS$_3$
10	90% Fe(xan)$_3$ + 10% Ni(xan)$_2$	120–180	68.7	NiS + FeS$_3$
11	Pure Fe(xan)$_3$	108–140	69.8	FeS$_3$
		200–240	5.3	FeS + Fe$_2$O$_3$ etc

TABLE 2

Thermal parameters calculated using different relations

Sample no	TG [a]		DTG			DTA		
			A [b]		B [c]	A [b]		B [c]
	n	E_a (kJ mole^{-1})	n	E_a (kJ mole^{-1})	L_a (kJ mole^{-1})	n	L_a (kJ mole^{-1})	L_a (kJ mole^{-1})
1	0.43	134.6	1.03	248.0	240.7	0.87	183.1	283.8
2	0.98	153.3	1.08	196.3	150.0	1.01	211.6	197.0
3	0.35	170.3	1.04	253.0	237.5	1.03	226.2	200.0
4	0.54	72.2	0.75	71.0	92.8	0.98	70.7	71.6
5	0.34	85.5	0.84	98.0	137.0	0.78	51.9	60.2
6	0.43	131.0	0.33	104.9	150.9	1.22	62.5	75.4
7	0.77	139.0	0.88	77.8	82.1	0.89	38.2	50.3
8	1.08	219.7	1.40	121.8	109.3	2.48	181.6	90.1
9	0.80	180.0	1.03	101.2	85.5	0.87	69.6	79.6
10	0.78	164.0	1.08	109.0	92.5	0.82	92.1	101.2
11	0.59	127.0	1.49	169.2	133.7	1.04	213.2	141.8

n = order of reaction; E_a = Activation energy

[a] using Freeman and Carroll's relation

[b] using Arrhenius relation

[c] using Borchardt and Daniels' relation

peak for structural transformations in the plateau region of a TG curve is peculiar for the three compositions, with increasing iron content from 50–70%. It appears that the structural and compositional changes have overlapped on each other producing a broad DTA peak extending beyond the limit of the TG loss curve. For the other compositions there is a multiplet structure of DTA peaks. This supports the idea of the formation of a definite composition over this region. Compared with the DTA curves of other compositions, those of these three compositions are simple in appearance.

(iii) The examination of the TG curves gives the changes observable due to the addition of increasing amounts of Fe(xan)$_3$ to Ni(xan)$_2$. For both pure complexes there is a clear single step loss with a steep slope. The temperature range of decomposition for the first step is between 50°C for Fe(xan)$_3$ and 80°C for the Ni(xan)$_2$, given in Table 1. Such a single step is observable for the TG curves of the mixtures containing 50–80%iron, but the slopes are not as steep as those for pure complexes. The DTG curves for all the remaining compositions are suggestive of two components in the decomposition process, as the two slopes are evident from TG curves. However, the two steps are not separated but appreciably overlap each other.

(iv) The plot of the starting temperature of the decomposition for different compositions exhibits a fairly good trend similar to the variation in boiling point of two miscible liquids [16]. Figure 3 shows a fall in temperature for the mixtures containing 0–40% iron. A small increase is observed for 50% iron composition and

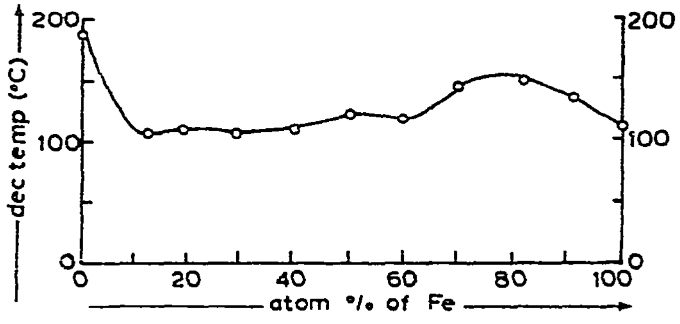

Fig 3 A plot of the decomposition temperatures of Fe(xan)$_3$ and Ni(xan)$_2$ against atom percent of Fe

again at the compositions of 70 and 80%. This shows a break in the general trend possibly because a different chemical process may be operating at these compositions.

Table 1 gives the TG data on the pure complexes and their mixtures. The probable composition of the residues has been ascertained on the basis of elemental analysis. Table 2 contains a comparative account of the kinetic parameters, such as the activation energy and the order of reaction calculated using the different relations referred to previously. Figure 4 presents a comparative account of these methods as a plot of activation energy against composition. The three methods do not agree in the magnitude of the activation energy but the data from any relationship do show a deviation at composition 50% and 60–80% of iron. The large deviation in the magnitude of E_a, may be due to the over simplification of the basic assumptions of each method and the inaccuracies in obtaining data for the different parameters. In Fig. 4, a subscript m signifies the E_a calculated manually, while c stands for computer fit, using the method of least squares; it has been found that the fitting parameter, χ (chi) was always less than 0.05.

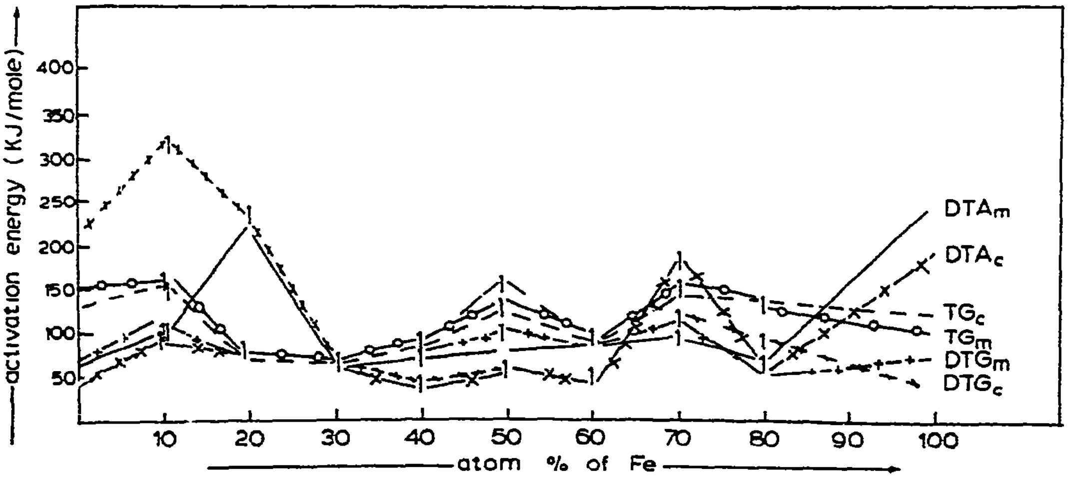

Fig 4 A plot of activation energy against composition

The inspection of the E_a values in Table 2 suggests that the trend observed in it is similar to the one reported [17].

It was worth attempting to elucidate the mechanism of these thermal decompositions. Satava [18] and Nair and Madhusudanan [19] have reviewed the different methods of thermal decompositions and proposed a unified approach to the elucidation of the different modes of decompositions on the basis of the fractions decomposing at unit time. The data on the fraction, α, of the substance decomposed at temperature T were obtained from TG curves and were manipulated using the proposed relations. The relation that gives a straight line plot for log $g(\alpha)$ against $1/T$ indicates the appropriate mechanism. It is found in the present work that the random nucleation mechanism [19] operates consistently with the Mampel equation. The agreement between the E_a values obtained from mechanism invoking and mechanism non-invoking relations was considered as the test for the correct operating mechanism (Table 3).

On the basis of the compositions of the residues (Table 1) the product obtained at 750°C containing 66% iron was analysed by Mossbauer and X-ray diffraction studies. Table 4 contains the data for Mossbauer parameters for a Fe:Ni composition of 2:1.

The product isolated at 750°C is expected to be nickel ferrite which is known to have Fe^{3+} (high-spin) configuration. The δ values observed in the present work are given in Table 4, and are found to fall in this compound (within an experimental error of ± 0.08 mm sec^{-1}) in the range of δ values for Fe^{3+} [20].

The confirmation of the formation of nickel ferrite may be seen from the close agreement between the X-ray parameters, d, for the compound prepared by the

TABLE 3

Comparative account for E_a calculated from various relations

Sample no	E_a (kJ $mole^{-1}$) calculated from						Remarks
	Non-mechanistic equation			Mechanistic equation			
	a	b	c	d	e	f	
1	134.6	248.0	240.5	317.0	139.0	99.0	e (a)
2	153.3	196.0	150.3	438.0	232.0	154.0	f (a and c)
3	170.3	233.0	237.5	247.0	127.0	86.0	d (b and c)
4	72.2	71.0	92.9	73.2	39.2	28.0	d (a and b)
5	85.5	98.0	137.0	99.0			d (b)
6	131.0	104.0	150.9	95.2	46.5	22.0	d (b)
7	139.0	77.8	82.1	82.0			d (b and c)
8	219.0	121.8	109.3	92.0			d (c)
9	180.0	101.0	85.5	133.0	86.1		e (c)
10	164.0	109.0	92.5	140.0	72.0		d (a)
11	127.0	169.0	133.7	283.0	131.0	81.9	e (a, c)

a, using Freeman and Carroll, b, using Arrhenius equation, c, using Borchardt and Daniels; d, using Mampel, e, using Avrami—I; f, using Avrami—II

TABLE 4

Mössbauer data for the system $Fe(xan)_3$–$Ni(xan)_2$—2:1

Set no	Chemical isomer shift (mm sec^{-1}) w r t iron (δ)	Quadrupole splitting (mm sec^{-1}) (ΔE)	Internal magnetic field KG	Comments
Subspectra A				
1	0.09		495.09	ΔE locked to zero Line width locked to 0.256 mm sec^{-1}
2	0.06	0.21	497.7	Line width locked to 0.256 mm sec^{-1}
3	0.11		496.1	ΔE locked to zero Line width locked to 0.256 mm sec^{-1}
Subspectra B				
1	0.44		504.69	ΔE locked to zero Line width locked to 0.32 mm sec^{-1}
2	0.47		503.8	ΔE locked to zero Line width locked to 0.32 mm sec^{-1}
3	0.45	0.32	505.8	ΔE locked to zero

xanthate decomposition method and those reported for nickel ferrite [21] given in Table 5.

In conclusion it may be stated that the study of the variation of kinetic parameters with composition for a binary system appears to be a useful means of investigating phase transformations. The formation of nickel ferrite at low temperatures may be due to the formation of an unstable homogeneous molten phase derived from complexes with a low melting point.

TABLE 5

X-Ray data for $NiFe_2O_4$ [$Fe(xan)_3 + Ni(xan)_2$ (2:1), heated to 750°C]

	1	2	3	4	5	6	7	8	9
Observed									
2θ	23.2°	25.6°	28.2°	38.4°	45.35°	47.4°	55.4°	69.5°	74.3°
θ	11.6°	12.8°	14.0°	19.2°	22.67°	23.7°	27.7°	34.75°	37.15°
sin θ	0.2011	0.2215	0.242	0.328	0.3855	0.4019	0.4648	0.5681	0.6039
d	4.817	4.37	4.0	2.94	2.512	2.425	2.083	1.725	1.6039
%	11.0	27.0	15.0	20.0	100.0	10.0	20.0	15.0	22.0
Reported									
d	4.82			2.95	2.51	2.41	2.08	1.70	1.60
%	7.0			20.0	100.0	5.0	23.0	13.0	33.0
hkl	111			220	311	222	400	422	511

ACKNOWLEDGEMENTS

We wish to thank Prof. V.K. Phansalkar, Head of the Department of Chemistry, for the facilities and encouragements given during the work. One of the authors (P.S.D.) is grateful to CSIR, New Delhi, for financial assistance during this work.

REFERENCES

1 G Gattaw and W. Behrendt, in A Senning (Ed), Topics in Sulphur Chemistry, Vol 2, George Thieme, Stuttgart, 1977
2 M A Khwaja, T J Cardwell and R J Magee, Anal Chim Acta, 64 (1973) 9
3 G W Watt and B J McCormik, J Inorg Nucl Chem., 27 (1965) 898
4 J P Fackler and W C Seidel, Inorg Chem , 8 (1969) 1631
5 K J Cavell, C G Seeney, J O Hill and R J Magee, Thermochim Acta, 5 (1973) 319
6 J P Fackler, W C Seidel and M Myron, Chem Commun , (1969) 1133
7 R Y. Salah and D K Straub, Inorg Chem , 13 (1974) 1559
8 Y Watanable and K Yamahate, Sci Pap Inst Phys Chem Res Jpn , 64 (1970) 71
9 A.I Vogel, A Text-book of Quantitative Inorganic Analysis, ELBS London 1975
10 S G Date, Ph D Thesis, Poona University, 1975
11 K J Standley, Oxide Magnetic Materials, Clarendon Press, Oxford, 2nd edn 1972
12 C Nickless, Inorganic Sulphur Chemistry, Elsevier, New York, 1968, p 718
13 A Blazak, Thermal Analysis, Van Nostrand–Reinhold, London, 1972
14 E S Freeman and B Carroll, J Phys Chem , 62 (1958) 394
15 H J Borchardt and F Daniels, J Am Chem Soc , 79 (1957) 41
16 W J Moore, Physical Chemistry, Orient Longman, New Delhi, 5th edn , 1972
17 M R Udupa, ITAS Newsreport, Indian Therm Anal Soc , 1979, p 14
18 V Satava, Thermochim Acta, 2 (1971) 423
19 C G.R Nair and P M Madhusudanan, Thermochim Acta 14 (1976) 373
20 N N Greenwood and T C Gibb, Mossbauer Spectroscopy, Chapman and Hall, London, 1971
21 ASTM INDEX (Card No 3-0875)